Compensation of Physiological Motion using Linear Predictive Force Control

Michel Dominici, Philippe Poignet, Etienne Dombre

2008 IEEE/RSJ International Conference on Intelligent Robots and Systems
Acropolis Convention Center
Nice, France, Sept, 22-26, 2008

Compensation of Physiological Motion using Linear Predictive Force Control

Michel Dominici, Philippe Poignet and Etienne Dombre

LIRMM-UMR CNRS, University of Montpellier II, F-34392 Montpellier cedex 5, France
emails:{dominici, poignet, dombre}@lirmm.fr

***Abstract*— This paper proposes a new approach to compensate the physiological motion, induced by respiration and heart beating, for robotized minimally invasive cardiac surgery. The control algorithm, based on a linear predictive control, uses the effort information applied on the heart by the instrument.**

I. INTRODUCTION

Nowadays, in order to access the heart to perform an intervention such as a Coronary Artery Bypass Graft (CABG), a great incision (of about $20\ cm$) is performed. The heart is stopped, blood circulation and respiration are performed by an external system (on-pump surgery). However, the use of a heart-lung machine implies more risks and a longer recovery time for the patient. Robotized mini-invasive cardiac surgery aims at minimizing the size of the incision and removing the cardiopulmonary bypass machine.

Nevertheless off-pump surgery implies another problem: the physiological motion. The two main sources of physiological motion inside the body are respiration and heartbeat. Respiration is the most important source of disturbances. It yields large cyclic displacements of several organs, mainly in the abdomen and thorax. Secondly, heartbeat motion involves high acceleration displacements. The sum of these motions can be very disturbing for the surgeon during the operation especially for surgical procedures requiring good precision (*e.g.*, needle insertion and suturing). Indeed, the gesture accuracy strongly depends on his/her ability to compensate these motions. Manual tracking of the complex heartbeat motion can not be achieved by a human without phase and amplitude errors [4].

A. Related Work in the Literature

The first approaches, to decrease heartbeat motion, used a mechanical device that constrains the motions of a small area on its surface by suction or pressure. Despite many improvements since the first version in the early $90's$, stabilizers still have some drawbacks: there is always residual motion, the suction device may produce injuries to the myocardium and the pressure device is not well suited for interventions which are located behind the heart.

Robotized surgery offers new means to efficiently circumvent such disturbances with lower risks and better accuracy. In [7], they performed experiments to track a marker attached to the surface of the heart with a 4 DOF robot using a highspeed vision system which measured the heart motion. The tracking error from the camera feedback system was relatively large (on the order of few millimeters in the normal direction). They demonstrated the feasibility of robotic tracking of fast heart movements and introduce the notion of "Heartbeat synchronization". This defines a control architecture where the surgeon can teleoperate a robot which is synchronized with the heart's motion.

Always using vision system, [5] and [8] performed motion canceling through the prediction of future heart motion using model based predictive controllers, in order to achieve higher precision tracking. A high-speed camera was used to measure heart motion. Their results indicated a tracking error variance on the order of 6-7 $pixels$ (approximately 1.5-$1.75\ mm$) in each direction of a $3D$ tracking task. Although it yielded better results than earlier studies using vision systems, the error was still very large to perform heart surgery like a coronary artery suture (the blood vessels have a $2\ mm$ or less diameter).

In [2], they proposed a force control (based on PI schema) coupled with an Iterative Learning Control where the error signal is filtered with varying cut-off frequency. The presented algorithm supposes that the perturbation is periodic. Since respiration is controlled by an external ventilator, the motion induced by respiration may be considered as periodic. This same hypothesis may however be too restrictive when it comes to the cardiac motion. Tests performed on an animated contact of a very simple periodic movement showed large errors.

In a recent work presented in [1], the control algorithms fuses information from multiple sources: mechanical motion sensors which measure the heart motion and sensors measuring biological signals. The control algorithm identifies the salient features of the biological signals and merge this information to predict the feedforward reference signal. This will improve the performance of the system since these signals are results of physiological processes which causally precede the heart motion.

B. Motivation and Methodology

Our work focuses on the mini-invasive cardiac surgery. The space available during the operation is limited and solutions requiring additional measuring instruments are only applicable for operations where a sternostomy is performed.

Preferably, heart motion compensation should be performed using instruments already available in common mini-invasive surgeries. The use of additional markers or sensors

placed on the heart surface reduces the workspace of the surgeon and consequently are of no interest.

Vision systems for tracking and compensating physiological motion have three major difficulties. First of all, a real time vision system to capture the heart motion in high speed is needed. This represents a great challenge for the design of the appropriate vision system.

In addition, the operation is performed in a confined environment. The tools must be in the visual field of view of the cameras, often occluding the region of interest. This results in a considerable deterioration of the tracking efficiency and consequently disturbs the overall motion compensation. A possible solution is the introduction of additional sources of information such as the electrocardiogram signal, in complement to the visual feedback.

Thirdly, the visual motion compensation does not take into account the effect of the gestures performed by the surgeon, which may modify radically the natural heart motion.

During free heart beating, individual points on the heart move as much as 7-10 mm. Although the dominant mode of the heart motion is in the order of 1-2 Hz, the measured motion of individual points on the heart during normal beating yields significant energy up to frequencies of 20 Hz. The tools need to track and manipulate a fast moving target with very high precision. The coronary arteries that are operated during CABG surgery range from 2 mm in diameter down to under 0.5 mm, which means the system needs to have a tracking precision in the order of 100 μm.

In our approach, we consider the two main sources of physiological motion: the breathing movement and the heart beat. Considering these motions as a source of perturbation, we propose a control system that allows a robot to move in a synchronized manner with the organ and to follow its motion, rejecting any perturbations. In this manner only the consign given by the surgeon is applied on the moving organ. Here we propose the use of force information given by a sensor located on the tool to retrieve the deformation caused by the surgeon's gestures. The controller has more precise information (workspace deformation and physiological motion), available in real time.

This paper explains the design and implementation of an intelligent control algorithm for robotic telechirugical systems, using a force control scheme coupled with a linear predictive loop which considers a simple internal model of the robot and its environment. Section II describes the experimental platform and its setup. Section III describes the control algorithms used in the compensation problem. The simulations results are presented in Section IV. Finally, the conclusions are given in Section V.

II. Experimental Setup

The experimental platform is composed by:

- a master station, the Phantom 1.5 haptic device
- a slave robot, the D2M2 robot designed for beating heart surgery experiments [3]. It has 5 DOF with direct drive technology providing fast dynamics and low friction.

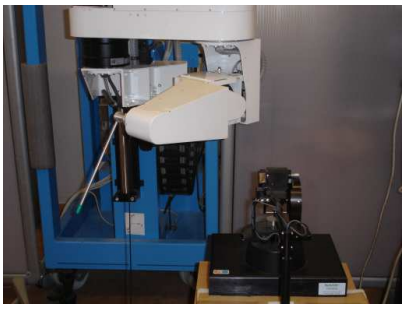

Fig. 1. Experimental platform: D2M2 robot and Phantom 1.5 haptic device

- a one DOF system, allowing to simulate the cardiac motion, controlled in position.

An ATI Mini 40 force sensor is attached to the D2M2 end-effector. The D2M2 is connected to a 500 MHz Intel Pentium 3 running under RTX/Windows 2000. The closed loop sampling time $h = 0.7$ ms, and the system time delay obtained experimentally is $T_d = 5h$. Master and slave stations are connected via UDP communication under Windows XP. A picture of the experimental setup is represented in Fig. 1.

A. Computed Torque

The dynamic model of the D2M2 robot is given by

$$M\ddot{q} + v(q,\dot{q}) + g(q) + J^T F_m = \tau \tag{1}$$

M and J are respectively the mass and Jacobian matrix. $v(q,\dot{q})$ is the vector of Coriolis and centripetal force, $g(q)$ is the gravity term and τ is the generalized torque acting on q. F_m denotes the measured contact force at the end-effector of the manipulator.

Using the operational space formulation, (1) can be written as

$$\Lambda_x \ddot{X}_s + V_x(q,\dot{q}) + g_x(q) + F_m = F_c \tag{2}$$

Λ_x, $V_x(q,\dot{q})$ and $g_x(q)$ are respectively the mass matrix, the Coriolis and centripetal force vector and the gravity term written in Cartesian coordinates [3], [6]. F_c denotes the commanded force. For the desired Cartesian-decoupled system

$$\ddot{X}_s = f^\star \tag{3}$$

F_c should be[1]

$$F_c = \hat{F}_m + \hat{V}_x(q,\dot{q}) + \hat{g}_x(q) + \hat{\Lambda}_x f^\star \tag{4}$$

Equation (3) represents the dynamics of a unitary mass for each Cartesien dimension. $f^\star$ is an acceleration (see (4)), being an input parameter.

The linearized and decoupled system in Cartesien space scheme is showed in Fig. 2. Introducing K_2 (damping loop), T_d (time delay of the system) and K_s (environment

[1]The expression of form "$\widehat{A}$" means "an estimation of the variable A"

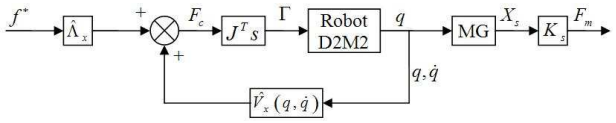

Fig. 2. Decoupled and linearized system in Cartesien space

stiffness), since T_d is small, the plant transfer function is given by

$$G(s) \approx \frac{K_s e^{-sT_d}}{s(s+K_2)} \tag{5}$$

Using the nominal value K_s (for the desired plant), the equivalent time representation is

$$\ddot{y}(t) + K_2\dot{y}(t) = K_s u(t - T_d) \tag{6}$$

where $y(t)$ is the plant output (Cartesian force at the robot's end-effector), and u is the plant input (force).

B. Global System

We use the haptic system developed in [3], its global scheme is represented in Fig. 3. It is composed by three parts:

- a master station, which includes the human and phantom. The phantom position X_{hp} scaled by β_p is compared to the end-effector position X_s, generating the 3D Cartesian force desired F_d through the virtual coupling K_v. The human arm perceives F_d scaled by β_f, which anticipates the real force.
- the system plant $G(s)$ linearized in Cartesian space has a function transfer given in (5).
- and a predictive controller described in the section below.

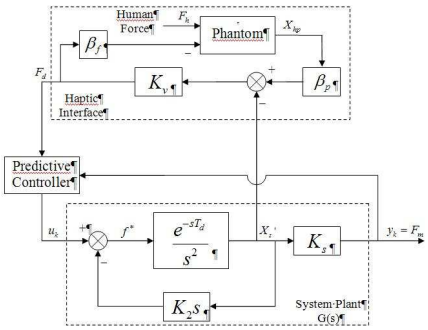

Fig. 3. Global control scheme with Linear Predictive Force Controller

III. Linear Predictive Controller

A. MPC Strategy

The methodology of the Model Predictive Control characterized by the following strategy, represented in Fig. 4:

- the future outputs for a determined horizon N, called the prediction horizon, are predicted at each instant t using the process model. These predicted outputs $\hat{y}(t+k|t)$[2] for $k = 1...N$ depend on the known values at the instant t (past inputs and outputs) and on the future control signals $u(t+k|t)$,$k = 0...N-1$, which will be sent to the system and then calculated.
- the set of future control signals is calculated by optimizing a determined criterion to keep the process as close as possible to the reference trajectory $w(t+k)$ (which can be the setpoint itself or a close approximation). This criterion takes the form of a quadratic function of the errors between the predicted output signal and the predicted reference trajectory. The control effort is included in the objective function. An explicit solution is calculated if the model is linear.
- only the first element of the sequence control calculated $u(t|t)$ is sent to the process. The horizon is displaced in the future and the algorithm is repeated with updated values.

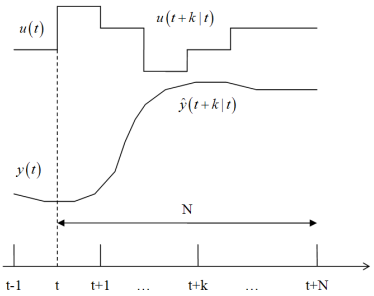

Fig. 4. MPC Strategy

B. Formulation of MPC

This section describes the MPC used for the experiments. The Fig. 5 shows the structure used. The process model is used to predict the future plant outputs, based on the past and current values and on the proposed optimal future control actions. These actions are calculated by the optimizer taking into account the cost function.

Defining the state variables $x_1(t) = y(t)$ and $x_2(t) = \dot{y}(t)$,

[2]The notation indicates the value of the variable at the instant $t+k$ calculated at instant t

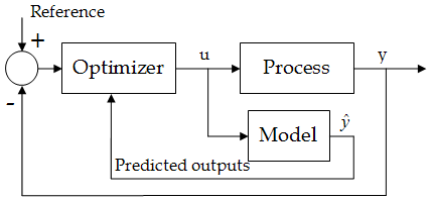

Fig. 5. Structure of MPC

(6) can be written as

$$\begin{bmatrix} \dot{x}_1(t) \\ \dot{x}_2(t) \end{bmatrix} = \begin{bmatrix} 0 & 1 \\ 0 & -K_2 \end{bmatrix} \begin{bmatrix} x_1(t) \\ x_2(t) \end{bmatrix} + \begin{bmatrix} 0 \\ K_s \end{bmatrix} u(t - T_d) \tag{7}$$

Discretizing (7) with sampling time h, the equivalent discrete time system is:

$$\begin{cases} x(k+1) = Ax(k) + Bu(k) \\ y(k) \quad\quad = Cx(k) \end{cases} \tag{8}$$

The predictions along the horizon are given by

$$\hat{y} = \Psi x(k) + \Upsilon u(k-1) + \Theta u \tag{9}$$

with

$$\begin{aligned} \Psi &= \begin{bmatrix} CA \\ CA^2 \\ \dots \\ CA^N \end{bmatrix} \quad \Upsilon = \begin{bmatrix} CB \\ \vdots \\ \sum_{i=0}^{N-1} CA^i B \end{bmatrix} \\ \Theta &= \begin{bmatrix} B & \cdots & 0 \\ C(AB+B) & \cdots & 0 \\ \vdots & \ddots & \vdots \\ \sum_{i=0}^{N-1} CA^i B & \cdots & B \end{bmatrix} \end{aligned} \tag{10}$$

The prediction (9) is composed of three terms, the first two depend on the past and the current states and are known at the instant k. The third depends on the vector of future control actions and is the key variable to be calculated.

The control sequence u is calculated by minimizing the objective function

$$J = \delta(\Theta u + \Psi\hat{x}(k) - w)^T(\Theta u + \Psi\hat{x}(k) - w) + \lambda u^T u \tag{11}$$

So the analytical solution is given by

$$u = (\delta\Theta^T\Theta + \lambda I)^{-1}\delta\Theta^T(w - \Psi\hat{x}(k) - \Upsilon u(k-1)) \tag{12}$$

where δ and λ are respectively the error and effort control weights. w is the future reference trajectory. Since receding horizon strategy is used, only the first element of the control sequence is sent to the plant and then all the computation is repeated in the next sampling time.

IV. Simulation And Robustness Test Results

A. Analysis of Physiological Motion Data

The motion data used are showed on the Fig.(6). This signal represents the cardiac and breathing motions (on the vertical axe) measured on a pig's beating heart. Its amplitude is of about 10 mm and lasts 15 s. A spectral analysis has been performed to evaluate the frequency components of the signal (see Fig.(7)). The first two components ($f_1 = 0.34$ Hz, and $f_2 = 0.68$ Hz) are due to the respiration activity. f_1 is equal to frequency imposed by the respiratory machine (20 cycles per minute) and f_2 is its harmonic. Heart activity provides the four other frequencies. $f_3 = 1.19$ Hz represents the heart beat cycle (around 70 beats per minute) and the three others are its harmonics.

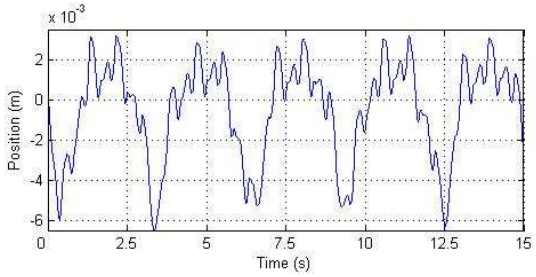

Fig. 6. Physiological motion data

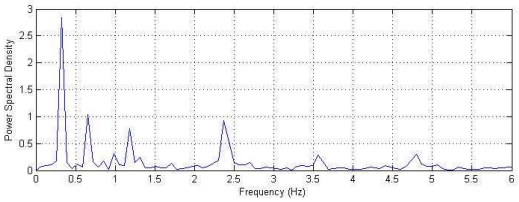

Frequency (Hz)	0.34	0.67	1.19	2.38	3.57	4.76
Density	70.9%	11.5%	5.9%	8.7%	1.2%	1.8%

Fig. 7. Spectral analysis of the physiological motion

B. Simulation Results

The simulation is executed on a 2.4 MHz Intel Pentium 4 running MATLAB R2007a.

Simulations are performed in order to evaluate the performance of the compensation algorithm with the Force Predictive Controller presented in the previous section. Three parameters are used to tune the algorithm: the horizon value N and the weight parameters. Even though tuned intuitively, the horizon does make a difference in the results. A longer horizon results in more accuracy of the tracking reference while the calculation time of the control sequence is longer. Therefore, a horizon must be chosen such that the control sequence can be calculated within one cycle of the control loop. For the simulations presented below, we use a constant horizon value of $N = 15h$.

The weight parameters δ and λ are used to modify the precision and the control effort respectively. An increase in δ implies the increase of both the accuracy and the control

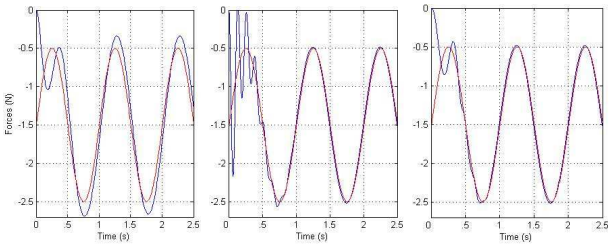

(a) (b) (c)

Fig. 8. Weighting parameters influence (realised on a fixed contact)

effort. More time is consequently needed to stabilise the robot near to the reference. We realised simulations to tune these parameters with a sinusoidal reference and a stable contact (see Fig.(8)). In (a) the parameters δ and λ are equal to 0.1 and 1 respectively. In (b) the error weight is equal to 5 and the control effort is equal to 0.1. And in (c), at the beginning, the error and effort control weights are equal to 0.01 and 5 respectively and when the effector applies a force near the reference, the parameters changed progressively to $\delta = 10$ and $\lambda = 0.1$.

Now that the weights are tuned, simulations are realised to evaluate the compensation algorithm. The motion data analysed above is used to animate the contact. Two kinds of reference, corresponding to desired force, are used : constant and variable reference.

In Fig.(9), the first three graphs display the applied force in blue and the desired force in red (set to $1\ N$ and varying from $0\ N$ to $12\ N$). During transient, the maximal error is about $248\ mN$ ($275\ \mu m$ with a contact stiffness of $900\ N/m$). After stabilisation (about $1\ s$), the maximal error is less than $24\ mN$, corresponding to a position error of about $27\ \mu m$. The fourth graph shows the positions of the contact (in red) and of the robot end-effector (in blue). The difference between the two is due to the D2M2 end-effector penetration in the contact, in order to apply the desired force. The last graph represents the torque applied on the motor of the robot for the variable reference, it's below the acceptable limit ($150\ N.m$).

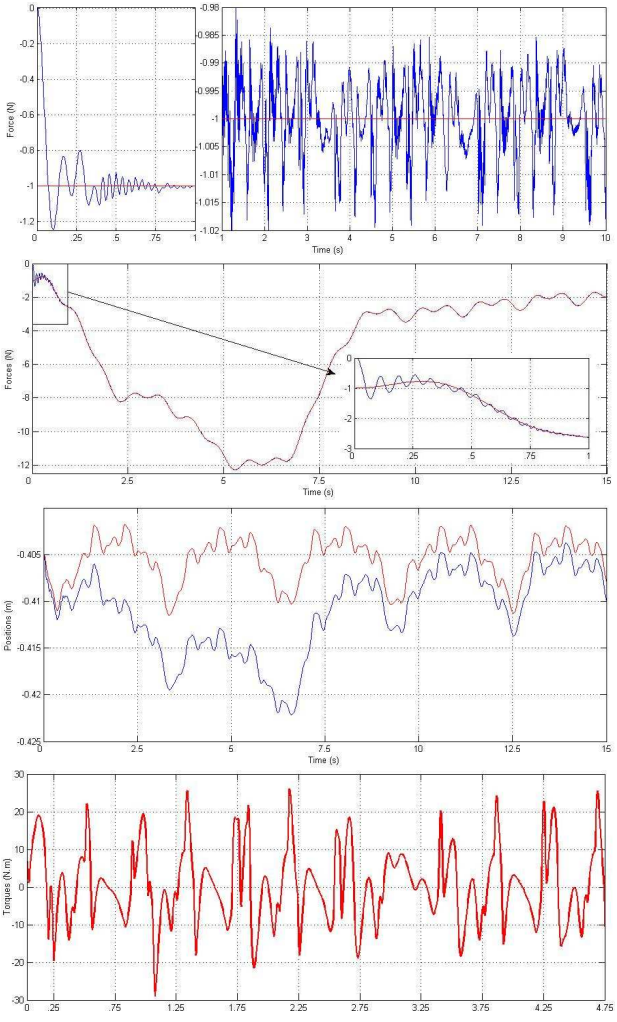

Fig. 9. Simulation results for a fixed/variable consign with animated contact

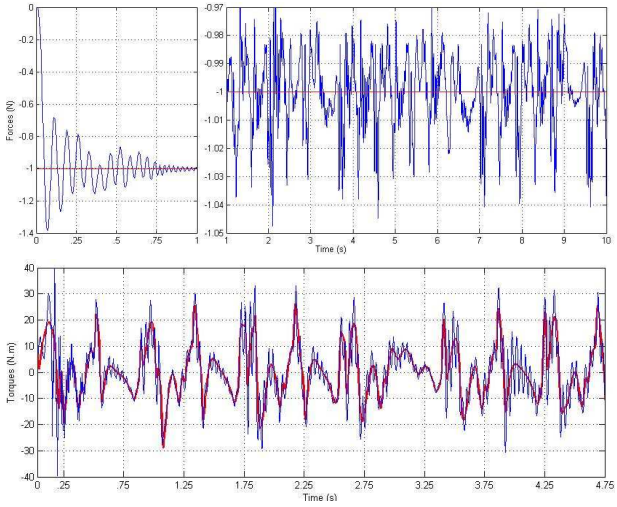

Fig. 10. Simulation results with identification and estimation errors

C. Robustness Test

To evaluate the robustness of the Predictive Force Control, two kinds of errors are added in the global system, identification and estimation errors. Firstly, we used the computed torque to linearize the system plant. We randomly vary the dynamic model parameters of about 40% of their nominal values to introduce indentification errors. Secondly, the environment stiffness K_s (robot and contact) is set to 20% of the stiffness contact value, $900\ N/m$, corresponding to a piece of boneless meat, introducing an estimation error. With these errors added, the model used by the predictive controller is not exactly the same of the system.

To compare with the simulations presented above, we used the sames references for the desired force. In Fig.(10), the first two graphs display the applied force in blue and the desired force in red (set to $1\ N$). During transient, the maximal error is about $390\ mN$ ($430\ \mu m$ with a contact stiffness of $900\ N/m$). After stabilisation (about $1\ s$), the maximal error is less than $48\ mN$, corresponding to a position error of about $53\ \mu m$. The last graph represents, in red, the torques for the nominal model without errors, and in blue, the torque for corrupted model.

D. Discussion of the Results

The first simulations, realised without errors introduced, show the good performances of the controller to realise breathing and heart beat motion compensation. For the

TABLE I

SIMULATIONS AND ROBUSTNESS TEST RESULTS

Physiological Motion Compensation		RMS Position Error (μm)		Max Position Error (μm)	
		Nominal model	*Corrupted model*	*Nominal model*	*Corrupted model*
Constant Consign ($1\ N$)	*before transient*	31.2	46.2	272.2	427.6
	after transient	4.7	5.8	26.9	30.1
Varying Consign ($1 - 10\ N$)	*before transient*	56.3	94.3	290.3	468.5
	after transient	8.3	10.5	35.4	38.9

robustness test, the same method (to tune the weight parameters) and motion data (used to animate the contact) are used. The identification and estimation errors added increase the position errors. In spite of the amplitude increase and the high frequency components apparence, the applied torque, with the corrupted system, is below the acceptable limit ($150\ N.m$). Among these results, the values of the RMS and Maximum Position Errors are summarized[3] in Table I.

V. CONCLUSIONS

This paper has presented an intelligent control algorithm for the physiological motion compensation in the domain of the mini-invasive cardiac surgery. It takes into consideration the breathing and heart beat motion without adding sensors or markers in the workspace to measure the motion. The information is given by a force sensor located on the tool. Depending to the workspace deformation and the physiological motion, this information is more precise and the data used by the controller is available in real time. The simulations show that this algorithm provides a significant compensation error decrease. Results are better than the best found in the literature [1].

Future work will focus on the improvement of the physiological motion compensation in two ways: on one hand, the weight parameters (here chosen intuitively) shall be tuned (in real time) as a function of the system's state. Secondly, the Linear Predictive Force Controller shall be included in the global scheme used in [9].

REFERENCES

[1] O. Bebek and M. C. Çavuşoğlu. Intelligent control algorithms for robotic assisted beating heart surgery. *IEEE Transactions on Robotics*, 23:468–480, June 2007.

[2] B. Cagneau, N. Zemiti, D. Bellot, and G. Morel. Physiological motion compensation in robotized surgery using force feedback control. In *Proc. of the IEEE Int. Conf. on Robotics and Automation (ICRA)*, pages 1881–1886, Roma, Italie, April 2007.

[3] R. Cortesão, W. Zarrad, P. Poignet, O. Company, and E. Dombre. Haptic control design for robotic-assisted minimally invasive surgery. In *Proc. of the IEEE Int. Conf. on Intelligent Robots and Systems (IROS)*, pages 454–459, Beijing, China, October 2006.

[4] V. Falk. Manual control and tracking-a human factor analysis relevant for beating heart surgery. *The Annals of Thoracic Surgery*, 74:624–628(5), 2002.

[5] R. Ginhoux, J. Gangloff, M. De Mathelin, L. Soler, M. M. A. Sanchez, and J. Marescaux. Active filtering of physiological motion in robotized surgery using predictive control. *IEEE Trans. on Robotics*, 21(1):67–79, February 2005.

[6] W. Khalil and E. Dombre. *Modeling, Identification and Control of Robots*. Hermes Penton Ltd, 3 edition, 2002.

[3] To validate the algorithms each simulation are repeated 50 times and the mean value is retained as a result.

[7] Y. Nakamura, K. Kishi, and H. Kawakami. Heatbeat synchronization for robotic cardiac surgery. In *Proc. of the IEEE Int. Conf. on Robotics and Automation (ICRA)*, volume 2, pages 2014–2019, Seoul, Korea, May 2001.

[8] J. Rotella. *Predictive Tracking of Quasi Periodic Signals for Active Relative Motion Cancellation in Robotic Assisted Coronary Artery Bypass Graft Surgery*. M.s. thesis, Case Western Reserve University, Cleveland, OH, USA, August 2004.

[9] W. Zarrad, P. Poignet, R. Cortesão, and O. Company. Towards teleoperated needle insertion with haptic feedback controller. In *Proc. of the IEEE Int. Conf. on Intelligent Robots and Systems (IROS)*, pages 1254–1259, San Diego, California, USA, November 2007.